THE JOURNAL OF PHYSICAL CHEMISTRY Letters

Letter

pubs.acs.org/JPCL

Photochemistry of Pheomelanin Building Blocks and Model Chromophores: Excited-State Intra- and Intermolecular Proton Transfer

Amal El Nahhas,*[,†] Torbjörn Pascher,[†] Loredana Leone,[‡] Lucia Panzella,[‡] Alessandra Napolitano,[‡] and Villy Sundström[†]

[†]Division of Chemical Physics, Lund University, Getingevagen 60, 22100 Lund, Sweden

[‡]Department of Chemical Sciences, University of Naples Federico II, Complesso MS Angelo, Via Cintia 4, I-80126 Naples, Italy

Supporting Information

ABSTRACT: Pheomelanins, the epidermal pigments of red-haired people responsible for their enhanced UV susceptibility, contain 1,4-benzothiazines and 1,3-benzothiazole as main structural components. Despite the major role played in pheomelanin phototoxicity, the photoreactivity of these species has so far remained unexplored. Static and time-resolved fluorescence spectroscopy was used to identify excited-state reactions of the two main pheomelanin benzothiazole building blocks, namely, the 6-(2-amino-2-carboxyethyl)-4-hydroxy-1,3-benzothiazole (BT) and the 2-carboxy derivative (BTCA) together with model chromophores lacking some of the ionizable functions. The results show that in aqueous buffer solution the OH at 4-position and the benzothiazole nitrogen atom control the photochemistry of both BT and BTCA via excited-state proton transfer to solvent (ESPT) and excited-state intramolecular proton transfer (ESIPT), while the amino acidic groups of the alanyl chain have a minor influence on the photochemistry. The ESPT and ESIPT produce several different excited-state ionic species with lifetimes ranging from ∼100 ps to ∼3 ns.

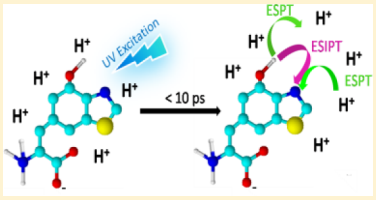

SECTION: Spectroscopy, Photochemistry, and Excited States

The characteristic phenotype of red-haired individuals of Celtic origin, with pale skin, blue-green eyes, and freckles, is due to the production of pheomelanin pigments.[1] The positive correlation between the red-hair phenotype and the UV-susceptibility trait, the high tendency to sunburn and the increased risk for skin tumors and melanoma[2] of these subjects, has been attributed to the poor antioxidant and photoprotective properties of pheomelanins compared with the dark eumelanins and the capacity of pheomelanin to act as photosensitizer inducing generation of reactive oxygen species (ROS) upon irradiation with UV light.[3−6] Following several studies on the reactivity of the putative biosynthetic intermediates[7,8] and chemical degradation analysis of pheomelanic tissues it now seems clear that pheomelanin structure includes benzothiazole moieties in addition to benzothiazine-related units. Recently, evidence has been obtained that a significant portion of benzothiazine units of pheomelanin in tissues undergoes ring contraction to benzothiazole on exposure to UVA.[9,10] It follows that characterization of the photoreactivity of benzothiazole moieties is central for dissecting the complex mechanisms underlying pheomelanin phototoxicity.

By combining steady-state and time-resolved fluorescence methodologies, we have now investigated the main benzothiazole building blocks of pheomelanin, that is, 6-(2-amino-2-carboxyethyl)-4-hydroxy-1,3-benzothiazole (BT) and 6-(2-amino-2-carboxyethyl)-4-hydroxy-1,3-benzothiazole-2-carboxylic acid (BTCA). Consideration of the structure of these molecules featuring several ionizable functional groups (heterocyclic N, aromatic OH, COOH, and amino acid functionalities) would suggest that excited-state proton transfer from/to solvent (ESPT) and excited-state intramolecular proton transfer (ESIPT) may play a crucial role. Such a behavior has also been observed in the case of structurally related molecules like the 2 (2′-hydroxyphenyl)-1,3-benzothiazole that has been the subject of detailed investigation.[11−14] To help identification of the excited-state processes we also investigated some model benzothiazoles like 2-methyl-1,3-benzothiazole (MB) and 4-hydroxy-6-methyl-1,3-benzothiazole (M-BT), having the chromophores of BT and BTCA but stripped of some of the functional groups like the hydroxyl group at the 4-position or the alanyl side chain at the 6-position (Chart 1).

While MB is commercially available, BT and BTCA were obtained by a one-pot multistep procedure starting from 5-*S*-cysteinyldopa.[15] A similar synthetic route was developed to obtain M-BT. All benzothiazole compounds were investigated in aqueous buffer solutions at selected pH values in the range 1−12 (values specified later for each molecule) as well as in methanol (MeOH). At the lowest pH studied the heterocyclic nitrogen of benzothiazole as well as the amino acidic amino group are mostly in the protonated form, and the aromatic and amino acidic COOH groups are not dissociated according to

Received: April 10, 2014
Accepted: May 22, 2014
Published: May 22, 2014

Chart 1. Molecular Structures of Pheomelanin Benzothiazole Building Blocks and Model Chromophores: 6-(2-Amino-2-carboxyethyl)-4-hydroxy-2*H*-1,3-benzothiazole (BT), 6-(2-amino-2-carboxyethyl)-4-hydroxy-2*H*-1,3-benzothiazole-2-carboxylic acid (BTCA), 2-Methyl-1,3-benzothiazole (MB), and 4-Hydroxy-6-methyl-1,3-benzothiazole (M-BT)

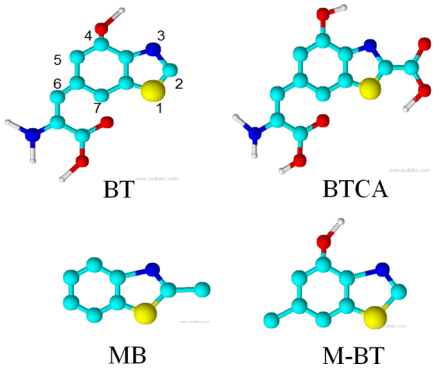

the pK_a reported in Table 1.[16−18] At the highest pH, all groups are deprotonated and BT is in its dianionic BT^{2-} form and BTCA is in its trianionic form $BTCA^{3-}$. (The notation used for the BT species discussed in this work is summarized in Table 1 according to their protonation states.)

Table 1. Ground-State pK_a Values of Functional Groups Occurring in the Benzothiazoles under Investigation and Notation Used for the Various Protonation States of 4-Hydroxy-1,3-benzothiazole

functional group (reference compound)	ground-state pK_a (ref)
NH^+ (4-hydroxy-1,3-benzothiazole)	1.84[15]
COOH (1,3-benzothiazole-2-carboxylic acid)	3.3[16]
COOH (tyrosine)	2.2[17]
NH_3^+(tyrosine)	9.1[17]
OH (4-hydroxy-1,3-benzothiazole)	8.8[18]
BT protonation state[a]	notation
OH; NH^+; NH_3^+; $COOH/COO^-$	BTH_2^{2+}
O^-; NH^+; NH_3^+; $COOH/COO^-$	BT^{-+}
OH; N; NH_3^+; $COOH/COO^-$	BT^+
O^-; N; NH_3^+; COO^-	BT^-
O^-; N; NH_2; COO^-	BT^{2-}

[a]Some species were combined in one disregarding their different COOH protonation states when it was not possible to distinguish between their individual contribution to the emission spectra.

Figure 1a,b displays the static absorption and fluorescence spectra of MB measured at pH 1 (in HCl solution), 2.5, 7, and 9.5 (phosphate buffer) and in MeOH. The absorption spectra of MB are very similar under all conditions examined, whereas the fluorescence spectra differ significantly. In MeOH, the fluorescence spectrum is characterized by a small Stokes shift ($\lambda_{max} \approx 330$ nm), suggesting no significant photochemistry and that emission originates from neutral MB. Similarly, at pH 9.5, the fluorescence spectrum peaks at $\lambda_{max} \approx 340$ nm (Figure 1b). At pH 1, the emission spectrum exhibits a red-shifted broad band centered at 410 nm (Figure 1b). On the basis of the pK_a = 1.84 of the heterocyclic nitrogen[16] (Table 1), at this pH, the dominating ground-state species is MBH^+ (88%, NH^+). Therefore, we assign the 410 nm fluorescence to protonated MB, MBH^+. At pH 2.5, almost the same fluorescence spectrum is observed as that at pH 1 (Figure 1b), although the ground-state species present are MBH^+ (∼18%) and MB (∼82%) (as judged by the pK_a = 1.84 of the heterocyclic N, Table 1). The fact that only MBH^+ fluorescence is observed at pH 2.5 (with 18% ground-state population) can be understood as a result of excited-state proton transfer from the solvent to the photoexcited MB. The heterocyclic nitrogen is known to be a photobase,[19] that is, a stronger base in the excited state. A Förster cycle calculation based on the fluorescence maxima of MB ($\lambda_{max} \approx 340$ nm at pH 9.5) and MBH^+ ($\lambda_{max} \approx 410$ nm) results in a $\Delta pK_a^* \approx 10$ pH units. Thus, it follows that proton transfer from the solvent to the thiazole nitrogen of the excited MB molecule is thermodynamically strongly favored. Consequently, we conclude that the 410 nm fluorescence band at pH 2.5 originates from both the 18% ground-state population of MBH^+ and the MBH^+ formed through ESPT from the solvent. The red-shifted MBH^+ fluorescence is similar to that of the hydroxyphenylbenzothiazole protonated form at 440 nm.[11,12] Time resolved fluorescence spectra of MB in pH 2.5 buffer (Figure 1c) exhibit a broad band centered at ∼430 nm (in agreement with steady-state fluorescence), characterized by single-exponential kinetics (Figure 1d), and therefore a single decay-associated spectrum (DAS, Figure S1 in the Supporting Information), having a decay time of 140 ps. This shows that MBH^+ is formed within the time resolution of the experiment (<10 ps). This and no detectable fluorescence at ∼340 nm of the excited major ground-state species (neutral MB) suggest that MBH^+ is formed along a N−H hydrogen bond already present in the ground state and therefore very fast. At intermediate pH 7 the fluorescence spectrum is dominated by the 340 nm band observed at pH 9.5 but also has a low amplitude of the pH 2.5 band at ∼430 nm (Figure 1b), supporting the picture of ESPT from the aqueous solvent to the ring nitrogen because at this pH the ground-state population of MBH^+ is negligible; the low amplitude is, of course, a result of the low proton concentration at this pH.

The absorption spectra of BT in sodium phosphate buffer at different pH values as well as in MeOH are shown in Figure 2a. The spectra in buffer at pH 2.5 and in MeOH are very similar. The absorption spectrum measured at pH 9.5 shows a shift of ∼4 nm for all of its spectral features compared with that at pH 2.5 and exhibits an extra band centered at ∼335 nm. On the basis of the pK_a values listed in Table 1, at this pH the majority of the BT molecules are in the deprotonated (O^-) form. The additional absorption band can therefore be assigned to this species. A similar red-shifted absorption band of hydroxyphenylbenzothiazole in aqueous ethanol solution, increasing in intensity with increasing pH, was attributed to the deprotonated (O^-) species, although in that structure a more extended delocalization of the anion compared with BT is expected.[20]

Steady-state emission spectra of BT in MeOH and aqueous buffer solutions in the pH range 2.5−12, measured upon 266 nm excitation, are shown in Figure 2b. A small Stokes shift is observed in MeOH (λ_{max} ∼390 nm) similarly to MB, suggesting that fluorescence originates from a position close to the Franck−Condon geometry and that no significant photochemistry occurs. Accordingly, the time-resolved fluorescence spectra and kinetics at selected wavelengths show a time-independent spectrum and wavelength-independent kinetics with a decay time of 255 ps (Figure S2 in the Supporting Information). The static fluorescence spectra in phosphate buffer solution at different pH values all exhibit large Stokes shifts (Figure 2b) and appear to be composed of at least two different emitting species with pH-dependent concentrations.

dx.doi.org/10.1021/jz500720g | J. Phys. Chem. Lett. 2014, 5, 2094−2100

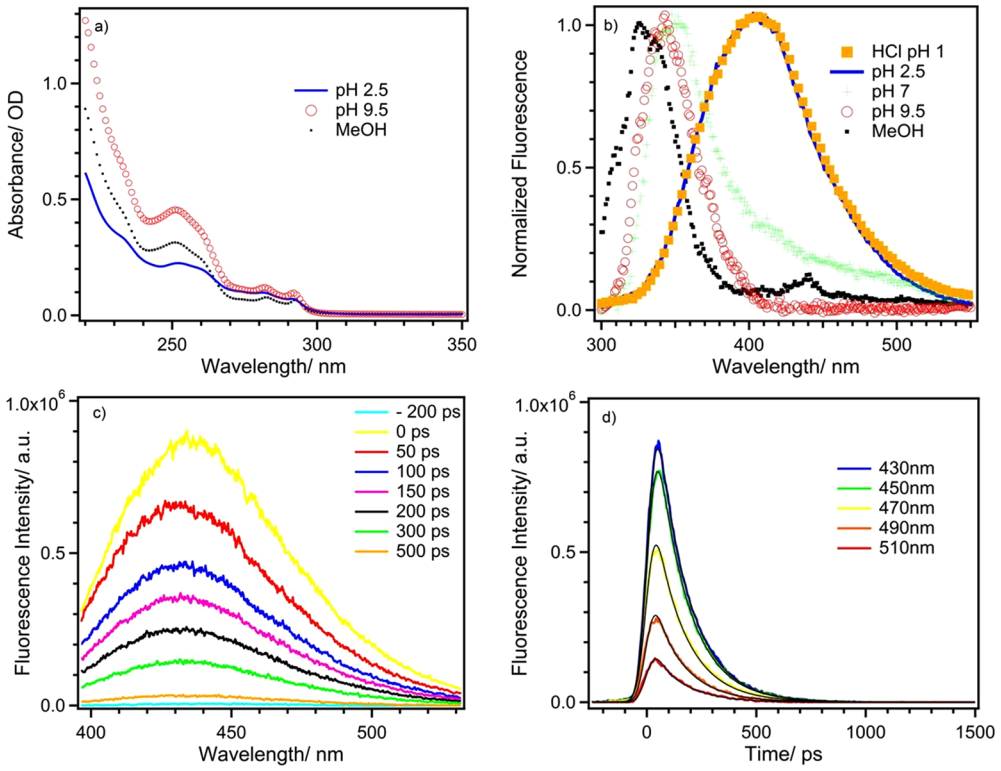

Figure 1. (a) Ground-state absorption and (b) steady-state fluorescence (upon 266 nm excitation) spectra of MB in MeOH and at pH 1, 2.5, 7, and 9.5. (c) Time-resolved fluorescence spectra of MB at pH 2.5. (d) Streak camera fluorescence kinetics of MB at pH 2.5 at several different wavelengths together with their fits, yielding a single exponential lifetime of 140 ps.

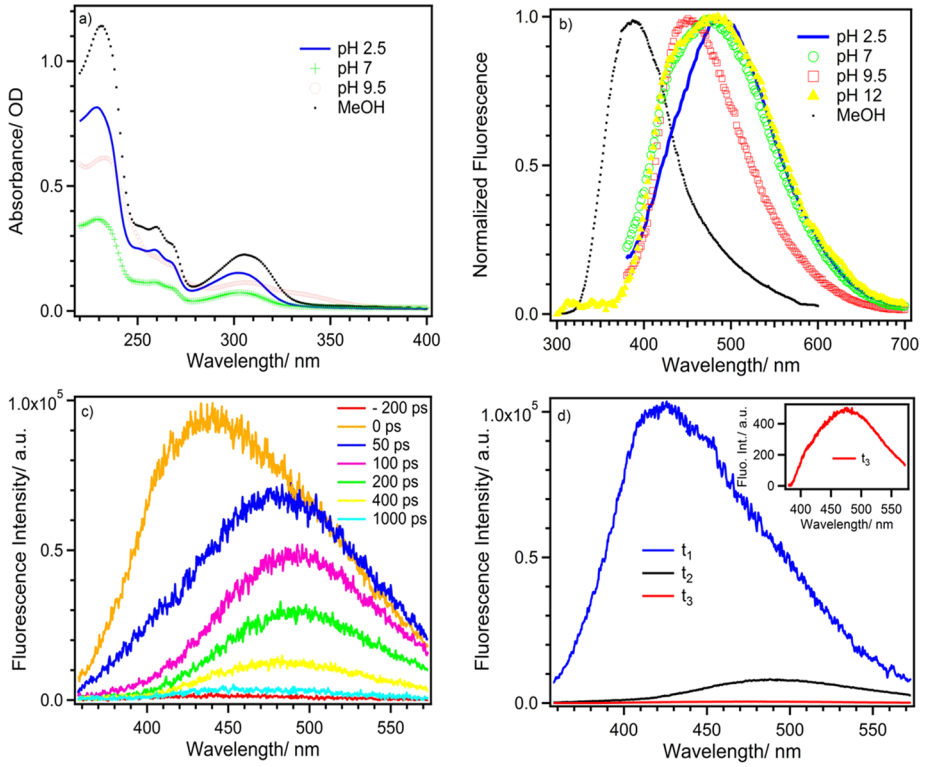

Figure 2. (a) Ground-state absorption and (b) steady-state fluorescence (upon 266 nm excitation) spectra of BT in MeOH and at various pHs. (c) Time-resolved fluorescence spectra of BT in aqueous buffer at pH 2.5. (d) DAS of the three components of BT in pH 2.5 buffer with lifetimes t_1 < 10 ps, t_2 = 230 ps, and t_3 = 1 ns.

At pH 12, dianionic BT^{2-} is the dominating ground-state species with only a small (<1%) contribution of monoanionic BT^{-} (Table 1). This sample composition gives rise to the fluorescence spectrum (Figure 2b) peaking at ∼480 nm with a

dx.doi.org/10.1021/jz500720g | J. Phys. Chem. Lett. 2014, 5, 2094−2100

shoulder at ~430 nm (Figure S3 in the Supporting Information), which we consequently assign to BT^{2-} (~480 nm) and BT^{-} (~430 nm) (more later). At pH 9.5, BT^{-} and BT^{2-} are the dominating species at about the same concentrations with a static fluorescence spectrum composed of the ~430 nm BT^{-} and ~480 nm BT^{2-} emission bands. (There is a minor (~17%) fraction of species with the 4-OH group protonated: OH; N; NH_3^+; COO^- and OH; N; NH_2; COO^-.)

At pH 2.5, the ground-state population is a mixture of species with heterocyclic N deprotonated (BT^{+}) at 82% of the total benzothiazole concentration and 18% protonated also at the heterocyclic nitrogen (BTH_2^{2+}), based on pK_a in Table 1. Nevertheless, the steady-state emission spectrum is not that of the BT^{+} but red-shifted by ~200 nm from the peak of the absorption band to λ_{max} ~490 nm (Figure 2b, Figure S3 in the Supporting Information). By analogy to what was observed for MB and as will be clear from the time-resolved fluorescence results (see later), this emission originates mainly from BTH_2^{2+} or BT^{-+} (At this point, we cannot distinguish between the fluorescence spectra of these two species. It appears that the protonation of the heterocyclic N is the determining factor for red-shifting the fluorescence to ~490 nm.) formed through excited-state proton transfer to the heterocyclic N. At pH 7, ground-state BT is in its neutral form and the static fluorescence spectrum exhibits a double-peak structure with maxima at ~430 and ~490 nm, that is, those of BT^{-} and BTH_2^{2+}/BT^{-+}. The ground state concentrations of BT^{-} and BTH_2^{2+} are negligible at pH 7, suggesting that these fluorescence bands must be a result of deprotonation of the 4-OH group due to ESPT/ESIPT and protonation of the heterocyclic N through ESPT from the solvent or ESIPT from the 4-OH, respectively.

The picture of excited-state proton transfer in BT hinted by the static fluorescence spectra may be substantiated with the help of time-resolved fluorescence results. In the pH range 2.5−9.5, the time-resolved fluorescence spectrum exhibits a fast <10 ps time-scale red shift from ~420 to ~500 nm. On a slower, several hundred picosecond time scale, the spectrum shifts back to ~450 nm and then decays without further change on the nanosecond scale (Figure 2c). This time evolution (Figure S4 in the Supporting Information) can be described by three pH-dependent DAS components having wavelength maxima approximately consistent with the static fluorescence bands in Figure 2b and characterized by exponential lifetimes: ~420 nm (<10 ps) (the <10 ps component is limited by the streak camera instrumental response, implying that the early time spectrum most likely has a maximum at somewhat shorter wavelength, ~400 nm). ~450 ± 20 nm (1 ns) (the very low amplitude of this component makes the determination of its wavelength maximum uncertain); and ~490 nm (230 ps) (Figure 2d). At pH 12, where BT^{2-} is the dominating ground-state species (~100%), the time-resolved fluorescence spectrum is dominated by a ~480 nm DAS component with a ~140 ps lifetime and only a very low amplitude of the ~450 nm DAS (1 ns). The time-resolved DASs can thus now be correlated to the various benzothiazole protonation states in the following manner: <10 ps (~400 nm) DAS−BT^{+}; 140 ps (~480 nm) DAS−dianionic BT^{2-}; 230 ps (~490 nm) DAS−BTH_2^{2+}/BT^{-+}; and 1 ns (~450 nm) DAS−monoanionic BT^{-}.

These correlations between BT protonation states, their fluorescence spectra, and associated lifetimes now allow us to suggest the following excited-state reaction scheme. Upon photoexcitation of BT, the excited state decays in <10 ps (~400 nm fluorescence) to form the excited-state BTH_2^{2+}/BT^{-+} and BT^{-}, which then decay with lifetimes of ~230 ps (490 nm fluorescence) and 1 ns (~450 nm fluorescence), respectively. The processes responsible for this are ESPT from the 4-OH group to the solvent for formation of the anion and 4-OH to heterocyclic-N ESIPT to form BT^{-+} or solvent to heterocyclic-N ESPT for BTH_2^{2+} formation. Similarly to MB, the latter process could significantly contribute at low pH. These processes control the fluorescence dynamics of benzothiazole at pH values where the 4-OH group is protonated (<9). At higher pH with this group deprotonated (4-O^-), no ESIPT and thus no significant protonation of the heterocyclic-N occurs, as is demonstrated by the much lower amplitude of 490 nm (230 ps) fluorescence at pH 9.5. (As a matter of fact, part of the ~200 ps amplitude here must be due to BT^{2-} (see previous).) At this pH, the proton concentration in solution is also low, making ESPT from the solvent negligible. At even higher pH 12, another red-shifted (~480 nm) fluorescence band appears, with almost the same maximum as that of BTH_2^{2+}/BT^{-+}, due to the ground-state concentration of BT^{2-} present at this pH. The fluorescence lifetime of this species is ~140 ps.

Förster calculations using the fluorescence spectra for BT^{+} (λ_{max} ≈ 390 nm) and BTH_2^{2+} (λ_{max} ≈ 490 nm) forms suggest that proton transfer from the solvent to the heterocyclic nitrogen is thermodynamically strongly favored, as in the case of MB. Using the fluorescence spectra in Figure 2b of BT^{+} and anionic BT^{-} forms, with maxima at ~400 and ~450 nm, respectively, the pK_a change in the excited state, ΔpK_a^*, can be estimated to be −6.3 pH units. Because pK_a of the 4-OH group is ~8.8, this suggests that ESPT occurs if the solution pH is >2.5. This is consistent with the lower spectral amplitude of BT^{-} fluorescence at pH 2.5 in both static and time-resolved spectra, as compared with pH 7 and 9.5 (Figures 2b,d). The excited-state proton transfers previously discussed are schematically summarized in Scheme 1.

The role of the amino acid side chain in the excited-state properties of BT was examined with the help of M-BT, lacking

Scheme 1. Summarizing the Reaction Model[a]

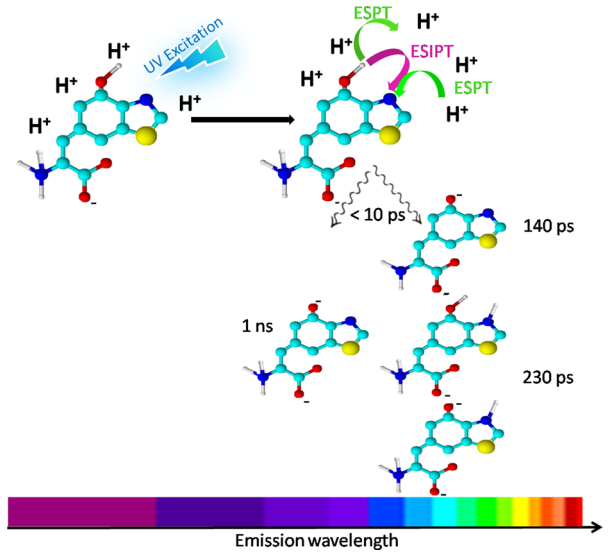

[a]Shown are the proton transfers occurring on the excited species at pH >3.

dx.doi.org/10.1021/jz500720g | J. Phys. Chem. Lett. 2014, 5, 2094−2100

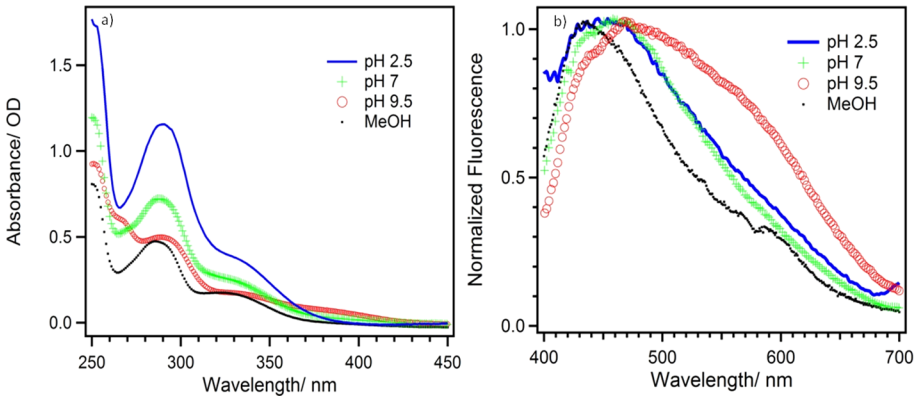

Figure 3. (a) Absorption and (b) steady-state fluorescence (upon 266 nm excitation) spectra of BTCA.

the alanyl side chain. The time-resolved fluorescence spectra and kinetics at both pH 2.5 (Figure S5 in the Supporting Information) and 9.5 (not shown) exhibit the same main pattern as that of BT: two spectral components characterized by maxima at 420−440 nm (10−20 ps) and ∼480 nm (100−150 ps). A component corresponding to the very low amplitude ∼1 ns component of BT^- could not be identified with certainty due to the higher noise in these measurements. These results support the picture previously obtained that the 4-OH and heterocyclic-N groups are the photochemical center of benzothiazole but that the protonation state of the NH_2/NH_3^+ group determines the excited-state lifetime of the BT anion (BT^- vs BT^{2-}).

The absorption spectra of BTCA in buffer solution at various pH values are shown in Figure 3a. At wavelengths <300 nm, the band structure is similar to that of BT but with somewhat shifted peak maxima and peak intensities varying with pH. In addition, there is absorbance extending further to the red, up to ∼400 nm, indicating the presence of additional low-lying transitions. The fluorescence spectrum of BTCA in MeOH is a single broad band with $\lambda_{max} \approx 440$ nm (Figure 3b) and is characterized by a relatively small Stokes shift, similarly to BT. In buffer solution at all pH values in the range 2.5 to 9.5, the fluorescence spectrum is broad and characterized by at least two bands at ∼450 and 600 nm, with a greatly increasing amplitude of the red band at pH 9.5 (Figure 3b). At this pH, the two COOH groups are fully deprotonated, the 4-OH is mostly deprotonated (82%), and the NH_2/NH_3^+ amino acid group at a ∼70/30 ratio was determined by its $pK_a = 9.11$. The red ∼600 nm shoulder of the fluorescence spectrum can consequently be associated with trianionic $BTCA^{3-}$ (COO^-, COO^-, O^-, NH_2). The corresponding fluorescence band was also observed for BT at ∼480 nm (previous); the fact that it is more red-shifted for BTCA makes it more easily distinguishable from the emission bands of the other species. As will be evident from the time-resolved measurements, the 450 nm band is a superposition of BTCA and $BTCA^{2-}$.

To fully disentangle the various contributions to the fluorescence spectrum, we turn to the time-resolved measurements. The time-resolved fluorescence of BTCA in the pH range 2.5−9.5 recovers DAS (Figure S6 in the Supporting Information) components and lifetimes that appear to be analogous to those identified for BT. A red-shifted component with a maximum at ∼580 nm and decay time of ∼100 ps spectrally coincides with the red shoulder in the static fluorescence spectrum appearing at pH 9.5. Therefore, it is straightforward to assign this DAS to the triple-anion $BTCA^{3-}$ with all functional groups deprotonated. The consequence of this is that the species with fluorescence maximum at ∼450 nm and ∼3 ns lifetime belongs to the anionic O^- species with the amino acid group in its zwitterionic (NH_3^+, COO^-) state. The ∼400−440 nm (∼10 ps) and ∼500 nm (∼280 ps) DAS components are assigned, analogously to BT, to the 4-OH and cationic (heterocyclic-N protonated) $BTCAH_2^{2+}$ forms. All of these spectral assignments are similar to those of BT in Scheme 1 and therefore not repeated.

The excited-state proton-transfer processes underlying the complex fluorescence behavior of both BT and BTCA can now be summarized in a few points. (i) No photochemistry occurs in methanol, as demonstrated by a small fluorescence Stokes shift and relatively long fluorescence lifetime (250−300 ps for BT), representing the sum of radiative and nonphotochemical radiationless processes of the benzothiazole core. (ii) In aqueous buffer solution, the OH at 4-position and the benzothiazole nitrogen atom control the photochemistry of both BT and BTCA via ESPT and ESIPT processes. (iii) The amino acidic groups of the alanyl chain have a minor influence on the photochemistry (but protonation state of the amino group determines the excited-state lifetime of anionic species). (iv) The ESPT and ESIPT produce several different excited-state ionic species with lifetimes ranging from ∼100 ps to ∼3 ns.

The findings here for BT and BTCA pheomelanin building blocks can now be compared with those of 5,6-dihydroxyindole (DHI) and 2-carboxy-5,6-dihydroxyindole (DHICA), the building blocks of eumelanin. On the monomer level there does not seem to be a dramatic difference between the various building blocks; in buffer solution they all exhibit ESPT or ESIPT processes (to a varying extent), and the resulting excited states decay on the hundreds of picoseconds to nanoseconds time scale.[21−25] In alcohol solution (methanol), these processes are much slower or completely stop.[23] Dimers and larger units of DHICA have remarkably different excited-state dynamics[21] compared with larger units of DHI: subpicosecond decay of the excited states through excited-state proton transfers.[25] This unique feature was correlated to the photoprotective functions of eumelanin. How incorporation of benzothiazole in pheomelanin backbone or its formation by benzothiazine ring contraction may change the excited-state dynamics is a question that future work is addressing.

The different fluorescence characteristics of eumelanin and pheomelanin is an issue of interest as a possible diagnostic tool for the detection of malignant transformation in melanocytes, which is associated with a switching from eumelanin to

dx.doi.org/10.1021/jz500720g | J. Phys. Chem. Lett. 2014, 5, 2094−2100

pheomelanin production.[26] The steady-state fluorescence of model synthetic pheomelanins has been previously[27] investigated, but up to now no interpretation of the species responsible for the phenomena has been provided because of the lack of information on the behavior of the putative building blocks inside the pigment. In this regard, the present investigation provide the first description of the steady-state and excited-state dynamics of the two main benzothiazole units of pheomelanin under conditions of relevance to the physiological process and provide a new groundwork for the interpretation of the photoreactivity of pheomelanin and the associated damages of the epidermal tissues.

■ ASSOCIATED CONTENT

Supporting Information

Experimental details and static and time-resolved fluorescence data at several more pH values and wavelengths are given as associated content. This material is available free of charge via the Internet at http://pubs.acs.org.

■ AUTHOR INFORMATION

Corresponding Author

*E-mail: amal.el_nahhas@chemphys.lu.se.

Notes

The authors declare no competing financial interest.

■ ACKNOWLEDGMENTS

Financial support is acknowledged from the Swedish Research Council, the Knut & Alice Wallenberg Foundation, and the European Research Council (Advanced Investigator grant 226136-VISCHEM). The work was carried out in the frame of the EuMelaNet program (http://www.espcr.org/eumelanet/).

■ REFERENCES

(1) Napolitano, A.; Panzella, L.; Leone, L.; d'Ischia, M. Red Hair Benzothiazines and Benzothiazoles: Mutation-Inspired Chemistry in the Quest for Functionality. *Acc. Chem. Res.* **2013**, *46*, 519−528.

(2) Rouzaud, F.; Kadekaro, A. L.; Abdel-Malek, Z. A.; Hearing, V. J. MC1R and the Response of Melanocytes to Ultraviolet Radiation. *Mutat. Res.* **2005**, *571*, 133−152.

(3) Chedekel, M. R.; Smith, S. K.; Post, P. W.; Pokora, A.; Vessel, D. L. Photodestruction of Pheomelanin: Role of Oxygen. *Proc. Natl. Acad. Sci. U.S.A.* **1978**, *75*, 5395−5399.

(4) Panzella, L.; Szewczyk, G.; d'Ischia, M.; Napolitano, A.; Sarna, T. Zinc-Induced Structural Effects Enhance Oxygen Consumption and Superoxide Generation in Synthetic Pheomelanins on UVA/Visible Light Irradiation. *Photochem. Photobiol.* **2010**, *86*, 757−764.

(5) Takeuchi, S.; Zhang, W.; Wakamatsu, K.; Ito, S.; Hearing, V. J.; Kraemer, K. H.; Brash, D. E. Melanin Acts as a Potent UVB Photosensitizer to Cause an Atypical Mode of Cell Death in Murine Skin. *Proc. Natl. Acad. Sci. U.S.A.* **2004**, *101*, 15076−15081.

(6) Wenczl, E.; Van der Schans, G. P.; Roza, L.; Kolb, R. M.; Timmerman, A. J.; Smit, N. P.; Pavel, S.; Schothorst, A. A. (Pheo)melanin Photosensitizes UVA-Induced DNA Damage in Cultured Human Melanocytes. *J. Invest. Dermatol.* **1998**, *111*, 678−682.

(7) Napolitano, A.; Memoli, S.; Crescenzi, O.; Prota, G. Oxidative Polymerization of the Pheomelanin Precursor 5-Hydroxy-1,4-benzothiazinylalanine: a New Hint to the Pigment Structure. *J. Org. Chem.* **1996**, *61*, 598−604.

(8) Greco, G.; Panzella, L.; Verotta, L.; d'Ischia, M.; Napolitano, A. Uncovering the Structure of Human Red Hair Pheomelanin: Benzothiazolylthiazinodihydroisoquinolines as Key Building Blocks. *J. Nat. Prod* **2011**, *74*, 675−682.

(9) Wakamatsu, K.; Nakanishi, Y.; Miyazaki, N.; Kolbe, L.; Ito, S. UVA-induced Oxidative Degradation of Melanins: Fission of Indole Moiety in Eumelanin and Conversion to Benzothiazole Moiety in Pheomelanin. *Pigm. Cell Melanoma Res.* **2012**, *25*, 434−445.

(10) Greco, G.; Wakamatsu, K.; Panzella, L.; Ito, S.; Napolitano, A.; d'Ischia, M. Isomeric Cysteinyldopas Provide a (Photo)degradable Bulk Component and a Robust Structural Element in Red Human Hair Pheomelanin. *Pigm. Cell Melanoma Res.* **2009**, *22*, 319−327.

(11) Becker, R. S.; Lenoble, C.; Zein, A. A Comprehensive Investigation of the Photophysics and Photochemistry of Salicylideneaniline and Derivatives of Phenylbenzothiazole Including Solvent Effects. *J. Phys. Chem.* **1987**, *91*, 3509−3511.

(12) Potter, C. A. S.; Brown, R. G.; Vollmer, F.; Rettig, W. Role of Twisted Intramolecular Charge-Transfer States in the Decay of 2-(2′-Hydroxyphenyl)benzothiazole following Excited-State Intramolecular Proton Transfer. *J. Chem. Soc., Faraday Trans.* **1994**, *90*, 59−67.

(13) Luber, S.; Adamczyk, K.; Nibbering, E. T. J.; Batista, V. S. Photoinduced Proton Coupled Electron Transfer in 2-(2′-Hydroxyphenyl)-Benzothiazole. *J. Phys. Chem. A* **2013**, *117*, 5269−5279.

(14) Douhal, A.; Sanza, M.; Tormo, L.; Organero, J. A. Femtochemistry of Inter- and Intramolecular Hydrogen Bonds. *ChemPhysChem* **2005**, *6*, 419−423.

(15) Greco, G.; Panzella, L.; Napolitano, A.; d'Ischia, M. Biologically Inspired One-pot Access Routes to 4-Hydroxybenzothiazole Amino Acids, Red Hair-Specific Markers of UV Susceptibility and Skin Cancer Risk. *Tetrahedron Lett.* **2009**, *50*, 3095−3097.

(16) Catallo, W. J.; Junk, T. Transformation of Benzothiazole in Estauarine Sediments. *J. Environ. Qual.* **2005**, *34*, 1746−1754.

(17) Todesco, P. E.; Vivarelli, P. Research on Benzothiazoles. VI. Acidity of Benzothiazole-2-carboxylic acid. *Gazz. Chim. Ital.* **1964**, *94*, 372−381.

(18) Berg, J. M.; Tymoczko, J. L.; Stryer, L. *Biochemistry*; W. H. Freeman and Company: New York, 2002.

(19) Feng, P. K.; Fernando, Q. Stabilities of Divalent Metal Complexes of 4-Hydroxybenzothiazole. *J. Org. Chem.* **1960**, *82*, 2115−2118.

(20) Potter, C. A. S.; Brown, R. G. Excited-State Intramolecular Proton Transfer in Polar Solutions of 2-(2′-Hydroxyphenyl)-benzothiazole. *Chem. Phys. Lett.* **1988**, *153*, 7−12.

(21) Gauden, M.; Pezzella, A.; Panzella, L.; Neves-Petersen, M.; Skovsen, E.; Petersen, S. B.; Mullen, K. M.; Napolitano, A.; d'Ischia, M.; Sundström, V. Role of Solvent, pH, and Molecular Size in Excited-State Deactivation of Key Eumelanin Building Blocks: Implications for Melanin Pigment Photostability. *J. Am. Chem. Soc.* **2008**, *130*, 17038−17043.

(22) Gauden, M.; Pezzella, A.; Panzella, L.; Napolitano, A.; d'Ischia, M.; Sundström, V. Ultrafast Excited State Dynamics of 5,6-Dhydroxyindole, a Key Eumelanin Building Block: Nonradiative Decay Mechanism. *J. Phys. Chem. B* **2009**, *113*, 12575−12580.

(23) Huijser, A.; Pezzella, A.; Hannestad, J. K.; Panzella, L.; Napolitano, A.; d'Ischia, M.; Sundström, V. UV-Dissipation Mechanisms in the Eumelanin Building Block DHICA. *ChemPhysChem* **2010**, *11*, 2424−2431.

(24) Corani, A.; Huijser, A.; Iadonisi, A.; Pezzella, A.; Sundström, V.; d'Ischia, M. Bottom- Up Approach to Eumelanin Photoprotection: Emission Dynamics in Parallel Sets of Water-Soluble 5,6-Dihydroxyindole-Based Model Systems. *J. Phys. Chem. B* **2012**, *116*, 13151−13158.

(25) Corani, A.; Pezzella, A.; Pascher, T.; Gustavsson, T.; Markovitsi, D.; Huijser, A.; d'Ischia, M.; Sundström, V. Excited-State Proton-Transfer Processes of DHICA Resolved: From Sub-Picoseconds to Nanoseconds. *J. Phys. Chem. Lett.* **2013**, *4*, 1383−1388.

(26) Leupold, D.; Scholz, M.; Stankovic, G.; Reda, J.; Buder, S.; Eichhorn, R.; Wessler, G.; Stucker, M.; Hoffmann, K.; Bauer, J.; et al. The Stepwise Two-Photon Excited Melanin Fluorescence Is a Unique Diagnostic Tool for the Detection of Malignant Transformation in Melanocytes. *Pigm. Cell Melanoma Res.* **2011**, *24*, 438−445.

(27) Nighswander-Rempel, S. P. Quantitative Fluorescence Spectra and Quantum Yield Map of Synthetic Pheomelanin. *Biopolymers* **2006**, *82*, 631−637.